

Climate-mediated shifts in temperature fluctuations promote extinction risk

Kate Duffy^{1,2*}, Tarik C. Gouhier³, and Auroop R. Ganguly^{1,4}

¹Sustainability and Data Sciences Laboratory, Department of Civil and Environmental Engineering, Northeastern University; Boston, Massachusetts 02115, USA.

²Bay Area Environmental Research Institute; Moffett Field, California 94035, USA.

³Department of Marine and Environmental Sciences, Marine Science Center, Northeastern University; Nahant, Massachusetts 01908, USA

⁴Pacific Northwest National Laboratory, Richland, WA 99354

*Corresponding author email: duffy.m.kate@gmail.com

Abstract

Climate-mediated changes in the spatiotemporal distribution of thermal stress can destabilize animal populations and promote extinction risk. Using quantile, spectral, and wavelet analyses of temperature projections from the latest generation of earth system models, we show that significant regional differences are expected to arise in the way that temperatures will increase over time. When integrated into empirically-parameterized mathematical models that simulate the dynamical and cumulative effects of thermal stress on the performance of 38 global ectotherm species, the projected spatiotemporal changes in temperature fluctuations are expected to give rise to complex regional changes in population abundance and stability over the course of the 21st century. However, despite their idiosyncratic effects on stability, projected temperatures universally increase extinction risk. These results show that population changes under future climate conditions may be more extensive and complex than the current literature suggests based on the statistical relationship between biological performance and average temperature.

Introduction

Biodiversity loss has been recognized as one of the top global risks by the World Economic Forum because it could erode or eliminate key ecosystem functions and services. Climate change is expected to surpass habitat loss as the leading threat to global biodiversity by the middle of the 21st century¹. Observed changes in the distribution and phenology of species have already been linked to climate fluctuations in numerous studies². Although conservation actions may ameliorate potential biodiversity loss, the success of these efforts depends on our ability to predict the response of ecological systems to environmental changes.

Most ecological impact studies to date have relied on statistical models such as bioclimate envelope approaches to determine how climate change will impact ecological populations³⁻⁶. Bioclimate envelope models are typically constructed by either mapping the geographical distribution of species to co-located temperature records via regression techniques or by building species' thermal profiles via empirical assessments of their performance across a range of

temperatures (i.e., thermal performance curves or TPCs)^{3,7}. These relationships between organisms and temperature are then used to predict the distribution of species under future thermal conditions projected under various climate change scenarios.

Despite their power and popularity, statistical approaches based on TPCs have inherent limitations in accounting for individual differences in age, habitat, and acclimatization history^{8,9}. Statistical approaches also can yield inaccurate predictions because they typically rely on mean annual conditions and thus ignore the influence of the temporal structure of temperature at finer scales. This is problematic because the nonlinear relationship between temperature and most metrics of biological performance essentially guarantees that the average organismal response will not be equivalent to their response to the average condition^{10–13}. Specifically, when an organism is exposed to a sequence of temperatures x , its performance at the average temperature $f(\bar{x})$ will differ from the average of its performance $\overline{f(x)}$. Temporal variation in temperature will either magnify ($\overline{f(x)} > f(\bar{x})$) or dampen ($\overline{f(x)} < f(\bar{x})$) the effects of its mean on organismal performance depending on the curvature of f (i.e., whether f is accelerating or decelerating¹⁰). In many cases, changes in temperature variability can be as or more important than changes in the climatological value^{14,15}. For example, climate-mediated changes in mean temperature alone were found to promote organismal performance in ectotherms, but accounting for the temporal variability of temperature dampened this effect and led to most species suffering a performance loss¹⁶.

Although the temporal structure of temperature can theoretically be incorporated into bioclimate envelope models by using finer-scale data, accounting for its dynamical effects on organisms is much more difficult because of the 'static' nature of these methods and their general inability to account for the cumulative effects of previous temperatures on organismal performance. However, theory has shown that such carry-over effects associated with the temporal structure or autocorrelation of temperature can interact with the magnitude of temperature variability to determine ecological persistence. Specifically, temporally autocorrelated variation tends to reduce extinction risk by decreasing the likelihood of catastrophic conditions under strong variation, whereas temporally autocorrelated variation tends to promote extinction risk under weak variation by increasing the likelihood that organisms will experience long stretches of poor conditions¹⁷. Additionally, analyses of historical observations and projections from previous generation climate models have found strong temporal trends in the variability and autocorrelation of temperature, suggesting the potential for a larger impact on ecological populations in the future^{18–21}. Overall, these empirical and theoretical results highlight the importance of quantifying changes in the mean, variability, and autocorrelation of temperature projected under climate change to predict their joint influence on ecological systems over the course of the 21st century. However, disparities in the scale of models in climate and ecology have hindered impact studies that consider the complexity of both underlying systems^{22,23}.

We briefly illustrate the potential for complex interactions between climate-mediated changes in the mean, variability, and autocorrelation of temperature to influence organismal performance by simulating the effects of synthetic temperature time series on the population growth rate r according to a species' TPC (Fig. 1, see Materials and Methods for modeling details). Predictably, performance under negligible temperature variation can be inferred directly from the mean of each species' TPC (Fig. 1b,c). However, when temporal variation in temperature is included in the model (i.e., standard deviation; shaded region), time-averaged performance can be considerably modified¹⁰, even overturning the species performance rankings based solely on constant temperature conditions (Fig. 1d,e). The temporal structure of temperature as measured by its autocorrelation also influences population dynamics by controlling the prevalence of long-term environmental fluctuations (Fig. 1f,g). To determine the impact of such changes over the course of the 21st century, we analyzed the latest generation of global climate models from the Coupled Model Intercomparison Project Phase 6 (CMIP6) in order to document spatiotemporal changes in three key aspects of air temperature (statistical distribution, variance, and temporal

autocorrelation). We analyzed the effects on ecological stability and persistence using simple strategic mathematical models to examine the hypothesis that even under ideal conditions, popular statistical methods can yield incorrect predictions about patterns of organismal performance when dynamical and cumulative temperature effects are ignored.

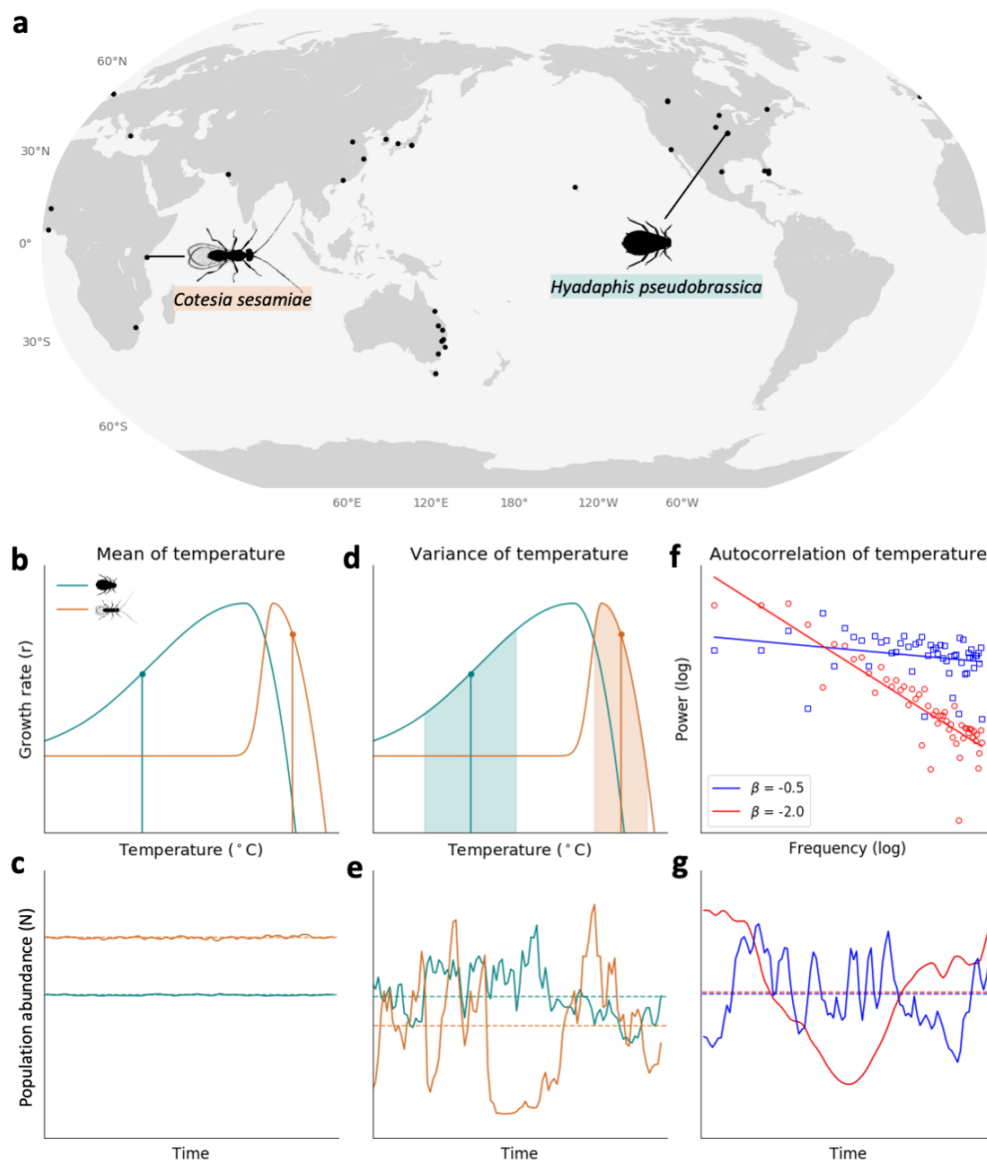


Figure 1. Effects of temperature mean, variance, and autocorrelation on organismal performance
a, Source locations of the 38 species whose thermal performance parameters of which were obtained from the Deutsch et al. (2008) dataset. *Cotesia sesamiae* is a tropical parasitoid wasp and *Hyadaphis pseudobrassicae* a temperate-zone turnip aphid. **b, c**, Thermal performance curves and population dynamics for *C. sesamiae* and *H. pseudobrassicae* under negligible temperature variation. **d, e**, Larger temperature variation (standard deviation shaded) alters mean response and may even overturn predictions of relative performance based on constant temperature conditions. **f**, The power spectrum of temperature with weak ($\beta = -0.5$) and strong ($\beta = -2.0$) temporal autocorrelation. **g**, Population dynamics of *Hyadaphis pseudobrassicae* under a greater degree of temporal autocorrelation exhibit longer-term fluctuations.

Results

We applied quantile regression to examine changes in the global and regional temperature distributions at each geographical location between 1850 and 2100 under the worst-case land use and emissions scenario, SSP5-8.5²⁴ (Fig. 2a). When averaging trends across regions, we found asymmetrical but uniformly positive trends across all quantiles, indicating that the entire temperature distribution is shifting upwards, but at rates that vary systematically across the distribution. In the Northern Hemisphere Extra-tropics (NHEX; 30°N to 90°N), the lowest quantile of the distribution ($\tau = 2.5\%$, 0.33 K decade⁻¹) is warming at twice the rate of the uppermost quantile ($\tau = 97.5\%$, 0.16 K decade⁻¹). The Southern Hemisphere Extra-tropics (SHEX; 90°S to 30°S) exhibit a similar pattern of disproportionate warming for the low quantiles ($\tau = 2.5\%$, 0.15 K decade⁻¹; $\tau = 97.5\%$, 0.10 K decade⁻¹). Conversely, in the Tropics (TROP; 30°S to 30°N), the upper quantiles of temperature are warming faster ($\tau = 97.5\%$, 0.14 K decade⁻¹) than the lower quantiles ($\tau = 2.5\%$, 0.10 K decade⁻¹). The magnitude of trends is greater in NHEX than in other regions. The more pronounced extra-tropical decrease in the incidence of cold events may benefit cold-limited species, including nuisance species, however, quantile trends also indicate increased positive skewness of the NHEX temperature distribution, which has been associated with declines in long term ecological performance¹⁶. Across all eight CMIP6 models that we analyzed and in all three latitudinal regions, trends in the tails of the distributions differ from the trends in the central tendencies, thus highlighting the importance of moving beyond mean temperature when predicting organismal performance.

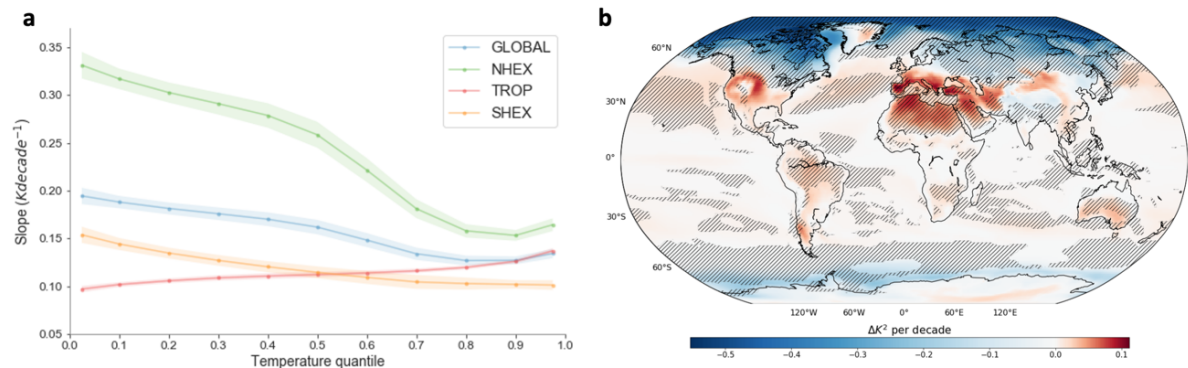


Figure 2. Mean trends in the statistical distribution of daily air temperature between 1850 and 2100. **a**, Trends in the percentile values of air temperature (K/decade) indicate asymmetrically warming temperature distributions in the Northern Hemisphere Extra-tropics (NHEX; 30°N to 90°N), the Tropics (TROP; 30°S to 30°N), the Southern Hemisphere Extra-tropics (SHEX; 90°S to 30°S), and the full globe (GLOBAL; 90°S to 90°N). Shaded bounds denote a 90% confidence interval based on eight CMIP6 models. **b**, Trends in the variance of daily air temperature (K²/decade) exhibit similarly complex regional patterns. The concurrent decrease of variability at high latitudes and increase at other latitudes suggests that temperature variation is becoming more spatially homogeneous in a warming world. Hashed contours indicate statistically significant inter-model agreement on the sign of the trend at the $\alpha = 0.05$ significance level.

Trends in the variability of temperature between 1850 and 2100 are predicted to exhibit similarly complex regional patterns (Fig. 2b). Variance is generally increasing across temperate and tropical land areas below 45°N, with regional exceptions including Asia. The strongest increases in variance are in the northern midlatitudes, including northern Africa, southern Europe, the Middle East, and the western United States. Variance is decreasing most rapidly in the high northern latitudes, especially in Canada and Russia²⁶. The concurrent decrease of variability at

high latitudes and its increase at other latitudes suggests that temperature variation, like mean temperature, is becoming more spatially homogeneous in a warming world. These findings are generally consistent with studies of the previous generation of climate models, which suggested increasing temperature variability in tropical countries²⁷ and decreasing variability in the northern mid- to high- latitudes²⁸. Trends at the regional level are congruent with quantile trends (Fig. 2a), which indicate a widening temperature distribution (increasing variance) in TROP, and a narrowing temperature distribution (decreasing variance) in NHEX and SHEX, as well as large scale changes in physical climate processes^{27–29}. The effects of these trends in temperature variation on ecological systems will depend on the geographical location and physiological properties of each species, with increasing variability either promoting or reducing performance based on its position relative to the inflection point of an organism’s TPC¹⁰.

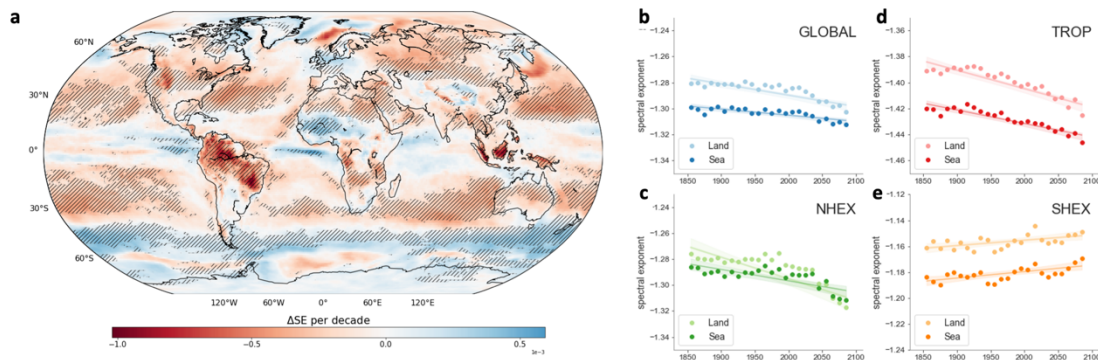


Figure 3. Increasing temporal autocorrelation in daily air temperature between 1850 and 2100.

a, Spatiotemporal trends in temporal autocorrelation suggest changes in the chronological sequence of temperature conditions, with increasing temporal autocorrelation (decreasing spectral exponent) at 80.04% of global land locations, excluding Antarctica. Hatched contours indicate statistically significant inter-model agreement on the sign of the trend at the $\alpha = 0.05$ significance level. **b-e**, Regional analysis indicates statistically significant increasing trends in temporal autocorrelation in NHEX and TROP and a statistically significant decreasing trend in temporal autocorrelation in SHEX. While sea environments generally exhibit a greater degree of temporal autocorrelation than land, in NHEX autocorrelation is increasing at a greater rate at land locations as to overturn this relationship by the end of the 21st century.

To better understand these spatiotemporal patterns, we used time-frequency decomposition via wavelet transform to resolve changes in the variability or power of temperature at annual timescales (2 day—2 year) and inter-to multiannual timescales (2—30 year; Extended Data Fig. 1). We found countervailing trends in scale-specific variability in the mid to high-northern latitudes. The magnitude of short-term variability is decreasing, while the magnitude of long-term variability is increasing. Arctic amplification, which is detectable in both observational data and climate simulations, has previously been suggested at the main driver of decreasing sub-seasonal variability at these latitudes²⁸. Meanwhile at the mid latitudes, variation at both annual and multiannual time scales is increasing, consistent with increasing variance at all periodicities. These scale-dependent changes in the temporal trends of temperature fluctuations could have important ecological implications. For instance, temperature fluctuations whose time scales are smaller than the generation time of organisms can have much greater impact on performance than larger-scale temperature fluctuations³⁰.

We computed the spectral exponent of the temperature time series at each geographical location to quantify spatiotemporal trends, with more negative exponents indicating greater temporal autocorrelation over a range of lags from 2 days to 10 years (Fig. 3a). We found increasing temporal autocorrelation (decreasing spectral exponent) at a majority of land locations (80%), excluding Antarctica, and sea locations (60%). Autocorrelation is increasing most rapidly in

equatorial land areas including the Amazon and the Southeast Asian islands with high inter-model agreement on the sign of the trend. Notable exceptions to the increasing trend in autocorrelation include Greenland, Western Africa, Western Europe, and parts of Central Asia. Generally, agreement between models is higher at mid-latitudes than in the polar zones or the tropics, where climate model bias and spread have historically persisted³¹. Regional analysis indicates statistically significant increasing trends in temporal autocorrelation in NHEX ($-1.12e^{-3}$ decade⁻¹, p-value=0.010), TROP ($-1.14e^{-3}$ decade⁻¹, p-value=0.001), and globally ($-0.54e^{-3}$ decade⁻¹, p-value=0.005), and a statistically significant decreasing trend in temporal autocorrelation in SHEX ($0.53e^{-3}$ decade⁻¹, p-value=0.009; Extended Data Fig. 2; Extended Data Table 1). The direction and significance of these trends are consistent across land and sea environments, although the spectral exponent is more negative for sea than land, likely due to the buffering effects of the ocean. In NHEX and TROP autocorrelation is increasing at a greater rate in land locations than sea locations while in SHEX autocorrelation is decreasing at similar rates between land and sea (Extended Data Table 2). A greater degree of temporal autocorrelation is associated with more gradual changes of state, and, even absent any changes in variance, results in longer durations spent under extreme conditions. A greater clustering of similar temperatures has been suggested to increase exposure to heat waves and cold snaps while decreasing the incidence of protective temporal refugia²⁰.

In the northern latitudes, variance and autocorrelation exhibit opposite temporal trends. The decreasing variance may be attributed to a decrease in high frequency variability and more rapid warming of the lower than upper quantiles of the temperature distribution. Studies of reanalysis data and observations have also implicated decreasing cold-season sub-seasonal variability and rapidly warming cold days in decreasing temperature variability in mid to high northern latitudes^{20,24,29}. Meanwhile, temporal autocorrelation in NHEX is increasing, a finding which has also been detected in the previous generation of climate models²⁰, weather station observations³³, and monthly reanalysis data¹⁹. As a result, variation at 2-day to 10-year periodicities is decreasing while temperature fluctuations are becoming more persistent, suggesting the increased probability of a series of homogeneous conditions. In contrast to the mid to high northern latitudes, variance and temporal autocorrelation show similar trends at most latitudes, that is, both variance and autocorrelation are increasing.

To better understand the independent and joint biological effects of these projected trends in the mean, variance, and autocorrelation of temperature on ecological systems, we used empirical thermal performance information from invertebrate ectotherms compiled by Deutsch et al. (2008). We extracted temperature time series from the eight CMIP6 climate models at geographical point locations corresponding to the source sites of the 38 species. A dynamical population simulation using species-specific temperature-dependent growth rates yielded time series of population abundance for the historical period (1950-2000) and the latter half of the 21st century (2050-2100). Using the eight climate simulations as replicates, we compared the historical and future periods to detect statistically significant temperature-driven changes in population abundance, stability (mean/standard deviation of abundance), and persistence (proportion of simulations where a species had a strictly positive final abundance).

Under the business-as-usual emission scenario (SSP5-8.5), population abundance increased for the plurality of species (18 of 38) and decreased for 10 species (Extended Data Table 3). Population abundance increased significantly for all TROP species (5 of 5) and for the majority (5 of 8) of SHEX species. In NHEX, outcomes were mixed with approximately equal proportions of species experiencing an increase in abundance, a decrease in abundance, and no significant change. NHEX population abundance followed latitudinal patterns, generally decreasing between 30°N and 45°N, and increasing above of 45°N. Under business-as-usual temperature changes, population stability increased for the plurality of species (16 of 38) and decreased for 10 species (Fig. 4a). Population stability increased or underwent no significant change for TROP species, while in the mid-latitudes (NHEX and SHEX), changes in stability were mixed. Additional analyses

showed that the trends in stability were mainly due to the emergence of two distinct dynamical regimes under climate change, with species either moving to a low-mean/low-variance mode or a high-mean/high-variance mode, particularly in the extra-tropics (Extended Data Fig. 4-5). These results were robust to un-normalized growth rates and equilibrium densities (Extended Data Fig. 2-3).

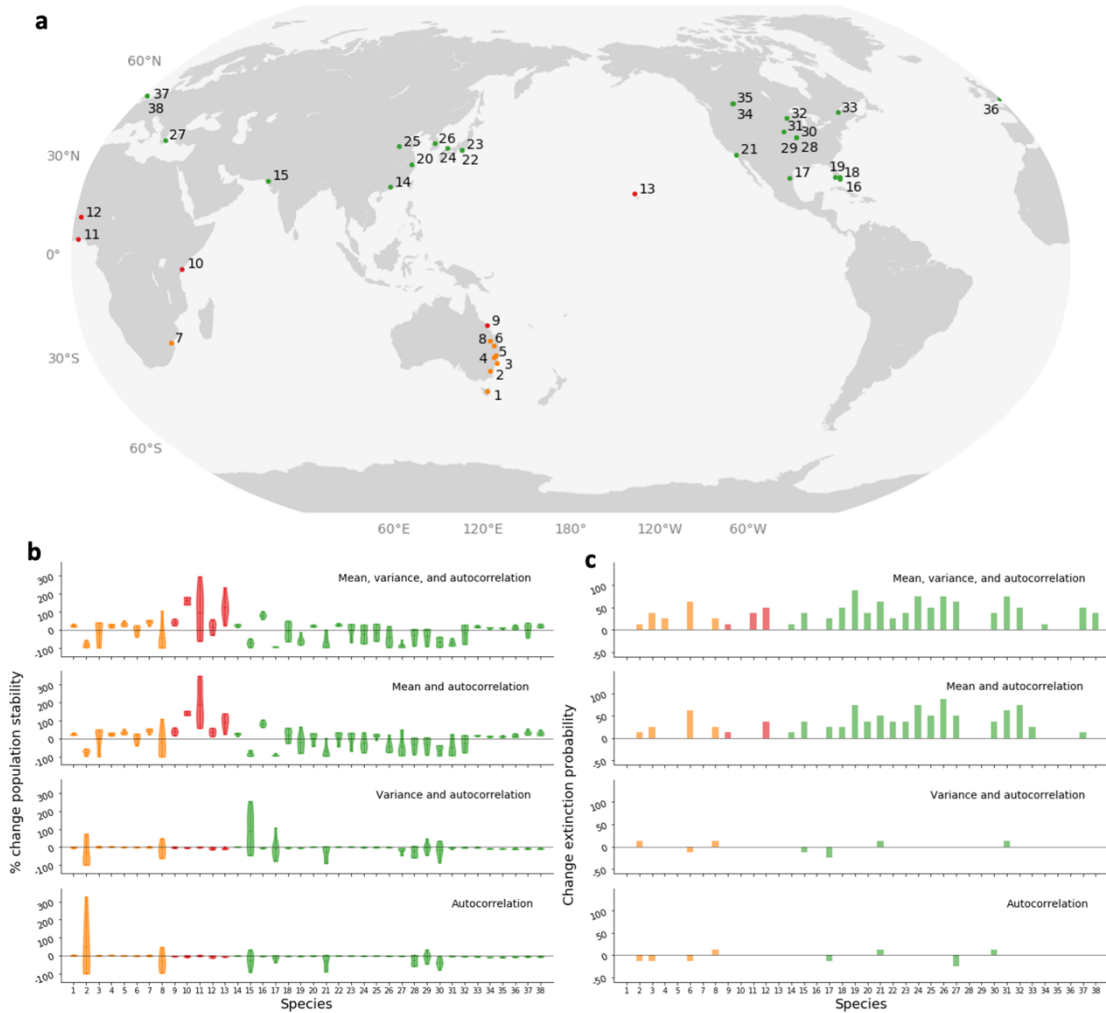


Figure 4. Temperature has idiosyncratic effects on stability but increases extinction risk globally. **a**, Source locations of the terrestrial ectothermic invertebrate species, numbered 1 (southern-most latitude) to 38 (northern-most latitude). Species are color-coded according to latitudinal region (SHEX; 90°S to 23°S; orange, TROP; 23°S to 23°N; red, NHEX; 23°N to 90°N; green) **b**, Percent changes in population stability (mean±standard deviation) between a historical reference period (1950-2000) and a future period (2050-2100) under multiple aspects of temperature change indicate greater risk to temperate than tropical species. Under a business-as-usual scenario, stability underwent a statistically significant increase for the plurality (16 of 38) of species and a statistically significant decrease for 10 species. **c**, Persistence probability underwent a quasi-universal decrease globally between the historical period (1950-2000) and a future period (2050-2100) under business-as-usual changes in temperature.

Many SHEX and NHEX species suffered performance losses (negative growth rates) during summers in their respective hemispheres, as they are generally less tolerant of hot temperatures than tropical species. For some temperate species, longer growing seasons and warmer winter temperatures offset the negative effect of the warmest part of the year, while others will suffer an overall performance loss³⁴. This is consistent with the suggestion that increases in summer heat stress would reduce overall fitness and increase fitness variation for many mid-latitude species³⁵. Our results suggest that temperate species may be at greater risk than tropical species as a result of warm days, even when annual mean temperature remains below the thermal optimum. The results contrast with those of a previous studies, which suggested based on hourly temperature records and monthly temperature anomalies that warming in the tropics would be more deleterious than warming in the mid-latitudes^{4,36}. Our results are more consistent with studies that predict a greater risk of performance loss for temperate species when accounting for climate-mediated changes in the mean and the variance of temperature¹⁶.

Our simulations indicated mean warming as the dominant driver of ecological impacts. Changes in temporal autocorrelation alone (mean temperature and variance held at historical levels) had no significant effects on population abundance and a significant destabilizing effect on just 3 NHEX species. Changes in temporal autocorrelation and variance (mean temperature held at historical levels) led to a decrease in population abundance in 2 NHEX species and a decrease in population stability in 5 NHEX species. These results suggest that NHEX species are more vulnerable to negative effects of changes in temperature variability than TROP or SHEX species. Finally, changes in mean and temporal autocorrelation (variance held at historical levels) led to increased population abundance in 19 global species and increased stability in 19 global species, versus 18 and 16 under business-as-usual projected changes in all three aspects of temperature. Thus, projected changes in temperature variability have a weak moderating effect on the positive effects of mean warming on population abundance and stability.

To determine how these complex changes in population abundance and stability translate to persistence, we quantified extinction risk as the proportion of the eight CMIP6 models for which population abundance declined below an arbitrarily small threshold of $1e-9$ at any point during the 50-year simulation (Fig. 4b). In our simulations, extinction risk increased between historical and future simulations for 25 species, did not change for 13 species, and decreased for 0 species under business-as-usual emission scenario. We found statistically significant increases in extinction risk globally (Mann–Whitney $U = 376$, $n_1 = n_2 = 38$, $p\text{-value} = 6e-5$) and in NHEX (Mann–Whitney $U = 150.5$, $n_1 = n_2 = 25$, $p\text{-value} = 5e-4$). These findings suggest that temperature changes have an overall negative effect on persistence, despite a largely positive or neutral impact on population abundance and idiosyncratic impacts on stability. Hence, although variability among climate models produces a wide range of changes in stability across species and geographical locations, uncertainty at the climate level yields consistent biological impacts in the form of a systematically higher extinction risk (Extended Data Fig. 6).

Discussion

Our demonstration of increased extinction risk under climate change is based on combining fine-scale temperature projections from the latest generation of Earth System Models with strategic dynamical models of population growth. Unfortunately, using more tactical dynamical models would require extensive species-, age-, and life-stage specific information about the effects of temperature fluctuations on population growth rates that is simply not available at the relevant scales. Tactical models would also need to consider thermoregulation³⁷, microclimate issues³⁸, acclimatization/adaptation⁸, partitioning of activity periods³⁹, and other mechanisms by which ectotherms could avoid extinction. Additionally, at a 1° spatial resolution, the climate data used in this study are much coarser than the microclimates experienced by individual organisms. Hence, our results should be viewed as a qualitative baseline prediction of how the spatiotemporal

distribution of extinction risk is likely to shift due to climate change rather than a quantitative forecast of when each species is likely to be extirpated from each geographical location.

Despite the inherent limitations of TPCs, the lack of obvious alternatives calls for strategies to make these approaches more robust to real-world conditions⁹, which is what we achieved by integrating more realistic, fine-scaled temperature variation into our predictive models than previous studies. Although bioclimate envelope approaches have been criticized for not accounting for important ecological factors such as species interactions and dispersal when attempting to predict the ecological effects of climate change^{40–43}, we have shown that even under ideal conditions when the influence of such factors can be assumed to be negligible, statistical frameworks that ignore the dynamical consequences of temperature variation are likely to yield inaccurate predictions about the impact of climate change on organisms. By their qualitative differences from previous results considering changes in mean temperature⁴, our results thus quantify how “black box” models using mean temperature can fail under nonstationary variation.

By bringing together climate data and a minimal, strategic, dynamical model from ecology we demonstrated a strong and systematic amplification of extinction risk in ectotherms due to projected changes in fine-grained temperature variability. Furthermore, our finding of greater risk to sub-tropical than tropical species highlights the importance of accounting for the dynamical effects of projected changes in the mean as well as variance of temperature over the course of the 21st century to accurately predict the response of ecological systems around the globe.

Methods

CMIP6 simulations

We obtained CMIP6 climate simulations for the historical forcing period (1850-2014) and future emissions scenario SSP5-8.5 (2015-2100) via the CMIP6 data portal (<https://esgf-node.llnl.gov/search/cmip6/>). Eight models from CMIP6 (AWI-CM-1-1-MR, BCC-CSM2-MR, CESM2, EC-Earth3, INM-CM5-0, MPI-ESM1-2-HR, MRI-ESM2-0, and NorESM2-MM) were selected based on availability of daily air temperature at surface (“tas”) at a 100 km nominal resolution at the time of download. While “tas” at sub-daily frequencies is available for some models, daily data was selected to maximize the ensemble size. We resampled all datasets to a common 1° by 1° grid spanning -90° to 90° latitude and 0° to 360° longitude, and to a standard calendar without leap years. Spatial regions were defined based on latitude as Northern Hemisphere Extra-tropics, 90°S to 30°S; Tropics, 30°S to 30°N; and Southern Hemisphere Extra-tropics, 30°N to 90°N.

Statistical analyses of climate data

Quantile regression

Trends in the percentile values global and regional temperature distributions were computed via quantile regression. Quantile regression can comprehensively model heterogenous conditional distributions, where the relationship between the quantiles of the dependent variable and the independent variable is different from the relationship between the mean of the dependent variable and the independent variable. We applied quantile regression to analyze trends with respect to time at various percentile values (P_{2.5}, P₁₀, P₂₀, P₃₀, P₄₀, P₅₀, P₆₀, P₇₀, P₈₀, P₉₀, P_{97.5}). Analyses were performed using the R package `quantreg`, with $\alpha = 0.1$ and the default Barrodale and Roberts method to return confidence intervals for the estimated parameters. To obtain the ensemble mean trends, we calculated the mean slope, upper bound, and lower bound across the eight climate models at each geographical location, then computed spatial averages for the full globe and three latitudinal regions.

Variance

Trends in the magnitude of temporal variation of air temperature were examined at each geographical location using a moving window approach. The temperature time series were divided into 10-year windows starting in years 1855 through 2085 so as not to combine historical and future simulations (pre- and post- 2015-01-01), and the variance of daily air temperature was calculated for each window. Windows were selected with no overlap to avoid statistical issues due to non-independence of estimates taken from partially overlapping time windows²⁰.

Scale-specific variability

Scale-specific variability was quantified using time-frequency decomposition. At each geographical location, a wavelet transform was applied to multi-model mean temperature using the R package *biwavelet*⁴⁴. From the resulting wavelet coefficient heatmap with time on the x-axis, period (scale) on the y-axis, and power on the z-axis, scale-averaged wavelet power was computed at annual (3 day-2 year), inter- to multiannual (2-30 year) periodicities. Scale-averaged power was regressed against time using Generalized Least Squares regression for the period 1850-2100 at each geographic location. To determine the robustness of results to the choice of period for scale averaging, we also performed analysis of trends separately at interannual (2-7 year) and multiannual (7-30 year) scales and found qualitatively similar results.

Temporal autocorrelation

The temporal autocorrelation of air temperature was quantified by calculating the spectral exponent at each geographical location²⁰. First, temperature was detrended by fitting a piecewise linear regression against time with Python package *pwlf* at each geographical location and extracting the residuals. The detrended temperature was divided into 10-year windows starting in years 1855 through 2085. Fourier transforms of each time series were computed via fast Fourier transform using the Python package *NumPy*. Periodograms were prepared with frequency on the x-axis and power spectral density on the y-axis. The spectral exponent, β , was calculated as the slope of the regression line relating log transformed power to log transformed frequency. β expresses the relative contributions of frequencies to the power spectrum. In the case of equal contribution from all frequencies, $\beta = 0$. Greater contribution from low frequencies than high frequencies results in a more negative value of β , and indicates greater temporal autocorrelation in the time domain.

Analysis of decadal trends

For each climate model, Generalized Least Squares (GLS) regression was used to detect statistically significant trends (p -value < 0.05) in variance and temporal autocorrelation with respect to time in the presence of potentially autocorrelated residuals. To measure inter-model agreement, we calculated the multi-model mean trend at each geographic location then assessed the proportion of models that agree with the sign of the multi-model mean trend. Inter-model agreement was considered as statistically significant at the $\alpha = 0.1$ level based on a binomial test. A one-way analysis of covariance (ANCOVA) was used to analyze the relationship between temporal autocorrelation and time while accounting for potential differences between land and sea environments. Statistically significant main effects and interactions were reported for p -value < 0.05 .

Modeling temperature impacts on ecology

Thermal tolerance data

We obtained experimentally derived thermal tolerance parameters for a set of terrestrial ectotherms ($n = 38$) published by Deutsch et al. (2008) and used them to predict physiological response to CMIP6 simulated temperature. The critical thermal maximum (CT_{max}), optimum temperature (T_{opt}), and sigma (σ) were used to estimate the thermal performance curve for each species based on its intrinsic rate of growth. Specifically, we used a numerical scheme whereby

the rise in performance up to T_{opt} was modeled as Gaussian and the decline beyond T_{opt} was quadratic^{4,45}

$$P(T) = \begin{cases} \exp\left[-\left(\frac{T-T_{\text{opt}}}{2\sigma_p}\right)^2\right] & \text{for } T \leq T_{\text{opt}} \\ 1 - \left(\frac{T-T_{\text{opt}}}{T_{\text{opt}}-CT_{\text{max}}}\right)^2 & \text{for } T > T_{\text{opt}} \end{cases} \quad [1]$$

This allowed negative growth rates to arise at high temperatures but growth rates were bound at zero at low temperatures. Because $P(T)$ is capped at 1 under this numerical scheme, $P(T)$ represents the relative fitness of each species based on its normalized maximum growth rate. However, scaling this relative or normalized maximum growth rate by a factor of 0.1 or 10.0 had very little quantitative and no qualitative impact on our results (Extended Data Fig. 3).

Isolation of temperature aspects

To isolate projected changes in mean temperature and variability, we transformed the future (2050-2100) time series to the historical (1950-2000) mean and/or standard deviation via z-score normalization. Working in 10 year moving windows between 2050 and 2100, each series x_i with mean m_1 and standard deviation s_1 was transformed to series y_i with mean m_2 and standard deviation s_2 :

$$y_i = m_2 + (x_i - m_1) \frac{s_2}{s_1} \quad [2]$$

According to the scenario, m_2 and s_2 were alternatively defined as [1] business-as-usual mean and standard deviation (“Mean, variance, and autocorrelation”), [2] business-as-usual mean and historical standard deviation (“Mean and autocorrelation”), [3] historical mean and business-as-usual standard deviation (“Variance and autocorrelation”), and [4] historical mean and standard deviation (“Autocorrelation”). Business-as-usual statistics refer to the properties of series x_i and confer no change to that aspect of the time series.

Population dynamical modeling

To model the effects of temperature change on the stability and persistence of global ectotherm populations, temperature dependence was integrated in the growth rate term of a population dynamical model⁴⁶. Basic population growth models fall into two categories: exponential and logistic. Both types of models are built as deterministic differential equations and are strategic in that they are designed to reveal general explanations for limited aspects of a system. The $r - \alpha$ logistic growth model incorporates a linear decrease in per capita growth rate as the population abundance increases, with the change in population calculated as

$$\frac{dN}{dt} = N(r_t - \alpha N) \quad [3]$$

with population size N , time t , temperature-dependent growth rate r_t , and density dependent crowding effect α . We extracted times series of daily temperature at the source locations for each species from the ensemble of eight climate simulations. Daily intrinsic growth rates were computed from temperature using Eqn. 1, incorporated into the $r - \alpha$ logistic growth model depicted in Eqn. 3, and the model was then numerically solved using the explicit Runge-Kutta method of order 5(4) implemented in the Python SciPy package in order to obtain daily population densities. Rather than delineating active periods, which may shift under climate change, we considered the full year to account for potential changes in fitness due to shifts in activity.

The sensitivity of the results to strong ($\alpha = 1$) and weak ($\alpha = 0.1$) self-regulation was examined and found to be extremely limited (Extended Data Fig. 2). We also assessed the sensitivity of our results to absolute rather than relative or normalized growth rates by scaling r_t by a factor of 0.1 or 10 in our simulations. Scaling r_t in this manner had very little quantitative and no qualitative impact on our results. This suggests that the effects of temperature fluctuations on changes in the spatiotemporal distribution of population size, stability, and extinction were not contingent upon the use of relative fitness (i.e., normalized growth rate) versus absolute fitness (i.e., growth rate scaled by a factor of 0.1 or 10).

Analysis of population changes

To quantify temperature-driven changes in ecological stability and persistence probability, we compared population sizes and dynamics between a historical period (1950-2000) and a future period (2050-2100). Here, we defined latitudinal regions according to traditional delineations in ecology: Northern Hemisphere Extra-tropics, 60°S to 23°S; Tropics, 23°S to 23°N; and Southern Hemisphere Extra-tropics, 23°N to 60°N.

Population abundance was computed as the mean population size (N) for a time period. Population stability was computed as the inverse of the coefficient of variation, or mean population divided by population standard deviation. Percent changes in population size and stability were computed for each of the climate models as $(\text{future} - \text{historical})/\text{historical} \times 100\%$ and plotted without outliers in Fig. 4. Statistically significant changes in population abundance and stability between the historical and future periods were identified via the Mann-Whitney U -test with the eight models as replicates.

Extinction probability was quantified as the proportion of ensemble simulations for which the population declined to zero during a 50-year simulation. Changes in persistence probability were calculated as the difference between future and historical persistence probability. Statistically significant changes in persistence probability were identified on a regional basis via the Mann-Whitney U -test.

Data availability

The CMIP6 simulation data used in this paper is available via the data portal <https://esgf-node.llnl.gov/search/cmip6/>. The ecology data is available for download at <https://doi.org/10.1073/pnas.0709472105>. Code to generate the results described above will be made available on GitHub following publication.

Acknowledgments

This work was supported by National Science Foundation grants (CyberSEES and CRISP).

References

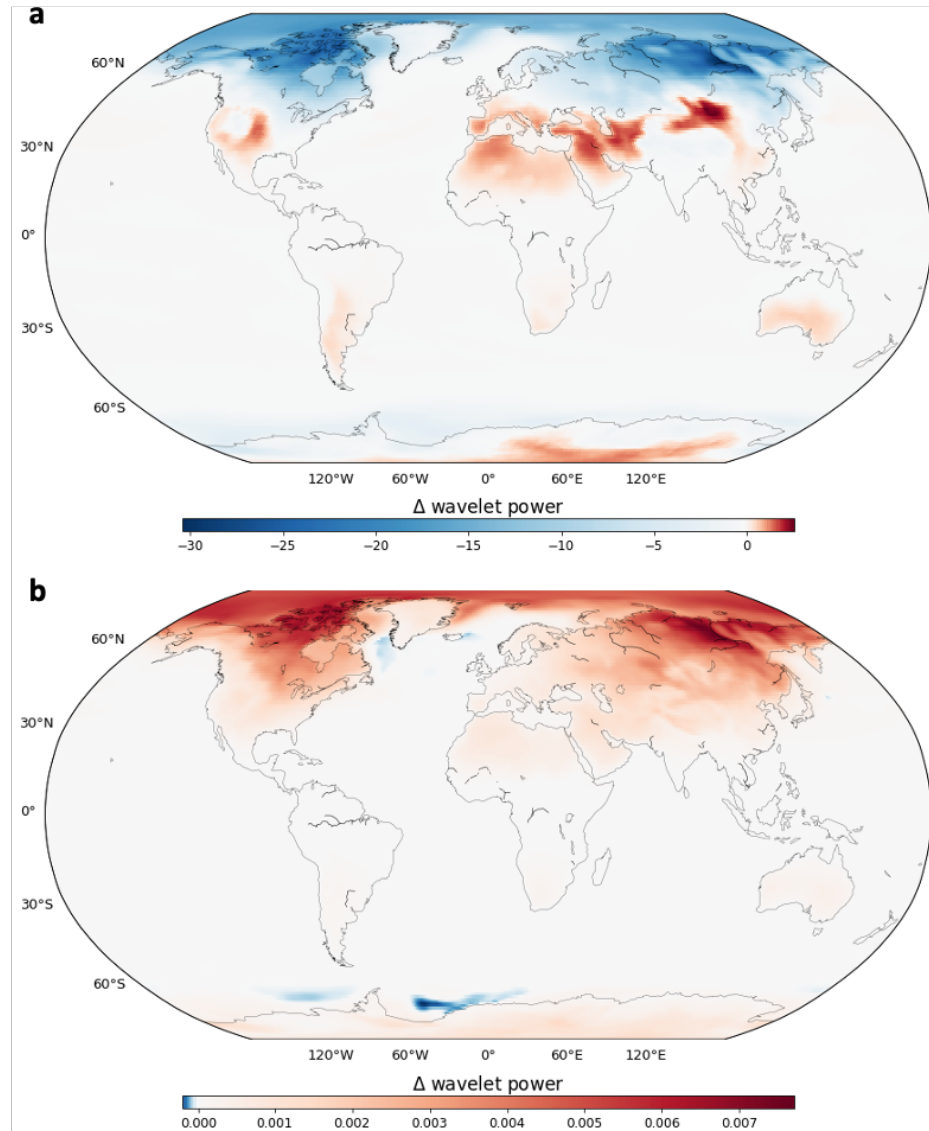
1. Bellard, C., Bertelsmeier, C., Leadley, P., Thuiller, W. & Courchamp, F. Impacts of climate change on the future of biodiversity. *Ecology Letters* **15**, 365–377 (2012).
2. Parmesan, C. Ecological and Evolutionary Responses to Recent Climate Change. *Annual Review of Ecology, Evolution, and Systematics* **37**, 637–669 (2006).
3. Pearson, R. G. & Dawson, T. P. Predicting the impacts of climate change on the distribution of species: are bioclimate envelope models useful? *Global Ecology and Biogeography* **12**, 361–371 (2003).
4. Deutsch, C. A. *et al.* Impacts of climate warming on terrestrial ectotherms across latitude. *Proceedings of the National Academy of Sciences* **105**, 6668–6672 (2008).
5. Cheung, W. W. L. *et al.* Projecting global marine biodiversity impacts under climate change scenarios. *Fish and Fisheries* **10**, 235–251 (2009).
6. Thuiller, W. *et al.* Consequences of climate change on the tree of life in Europe. *Nature* **470**, 531–534 (2011).
7. Angilletta, M. J. *Thermal Adaptation: A Theoretical and Empirical Synthesis*. *Thermal Adaptation* (Oxford University Press, 2009).
8. Somero, G. N. The physiology of climate change: how potentials for acclimatization and genetic adaptation will determine ‘winners’ and ‘losers’. *Journal of Experimental Biology* **213**, 912–920 (2010).
9. Sinclair, B. J. *et al.* Can we predict ectotherm responses to climate change using thermal performance curves and body temperatures? *Ecology Letters* **19**, 1372–1385 (2016).
10. Ruel, J. J. & Ayres, M. P. Jensen’s inequality predicts effects of environmental variation. *Trends in Ecology & Evolution* **14**, 361–366 (1999).
11. Lawson, C. R., Vindenes, Y., Bailey, L. & Pol, M. van de. Environmental variation and population responses to global change. *Ecology Letters* **18**, 724–736 (2015).
12. Denny, M. The fallacy of the average: on the ubiquity, utility and continuing novelty of Jensen’s inequality. *Journal of Experimental Biology* **220**, 139–146 (2017).
13. Denny, M. Performance in a variable world: using Jensen’s inequality to scale up from individuals to populations. *Conservation Physiology* **7**, coz053 (2019).
14. García-Carreras, B. & Reuman, D. C. Are Changes in the Mean or Variability of Climate Signals More Important for Long-Term Stochastic Growth Rate? *PLOS ONE* **8**, e63974 (2013).
15. Benedetti-Cecchi, L., Bertocci, I., Vaselli, S. & Maggi, E. Temporal Variance Reverses the Impact of High Mean Intensity of Stress in Climate Change Experiments. *Ecology* **87**, 2489–2499 (2006).

16. Vasseur, D. A. *et al.* Increased temperature variation poses a greater risk to species than climate warming. *Proc. R. Soc. B* **281**, 20132612 (2014).
17. Schwager, M., Johst, K. & Jeltsch, F. Does Red Noise Increase or Decrease Extinction Risk? Single Extreme Events versus Series of Unfavorable Conditions. *The American Naturalist* **167**, 879–888 (2006).
18. Meehl, G. A. More Intense, More Frequent, and Longer Lasting Heat Waves in the 21st Century. *Science* **305**, 994–997 (2004).
19. Lenton, T. M., Dakos, V., Bathiany, S. & Scheffer, M. Observed trends in the magnitude and persistence of monthly temperature variability. *Sci Rep* **7**, 5940 (2017).
20. Di Cecco, G. J. & Gouhier, T. C. Increased spatial and temporal autocorrelation of temperature under climate change. *Sci Rep* **8**, 14850 (2018).
21. Li, J. & Thompson, D. W. J. Widespread changes in surface temperature persistence under climate change. *Nature* **599**, 425–430 (2021).
22. Lembrechts, J. J. *et al.* Comparing temperature data sources for use in species distribution models: From in-situ logging to remote sensing. *Global Ecology and Biogeography* **28**, 1578–1596 (2019).
23. Potter, K. A., Arthur Woods, H. & Pincebourde, S. Microclimatic challenges in global change biology. *Global Change Biology* **19**, 2932–2939 (2013).
24. O'Neill, B. C. *et al.* The Scenario Model Intercomparison Project (ScenarioMIP) for CMIP6. *Geosci. Model Dev.* **9**, 3461–3482 (2016).
25. Dukes, J. S. *et al.* Responses of insect pests, pathogens, and invasive plant species to climate change in the forests of northeastern North America: What can we predict? This article is one of a selection of papers from NE Forests 2100: A Synthesis of Climate Change Impacts on Forests of the Northeastern US and Eastern Canada. *Can. J. For. Res.* **39**, 231–248 (2009).
26. Hansen, J., Sato, M. & Ruedy, R. Perception of climate change. *Proceedings of the National Academy of Sciences* **109**, E2415–E2423 (2012).
27. Bathiany, S., Dakos, V., Scheffer, M. & Lenton, T. M. Climate models predict increasing temperature variability in poor countries. *Sci. Adv.* **4**, eaar5809 (2018).
28. Screen, J. A. Arctic amplification decreases temperature variance in northern mid- to high-latitudes. *Nature Clim Change* **4**, 577–582 (2014).
29. Stouffer, R. J. & Wetherald, R. T. Changes of Variability in Response to Increasing Greenhouse Gases. Part I: Temperature. *Journal of Climate* **20**, 5455–5467 (2007).
30. Gouhier, T. C. & Pillai, P. Commentary: Nonlinear averaging of thermal experience predicts population growth rates in a thermally variable environment. *Front. Ecol. Evol.* **7**, (2019).

31. Tian, B. & Dong, X. The Double-ITCZ Bias in CMIP3, CMIP5, and CMIP6 Models Based on Annual Mean Precipitation. *Geophysical Research Letters* **47**, e2020GL087232 (2020).
32. Symon, C. Arctic Climate Impact Assessment - Scientific Report. *Cambridge University Press* (2005).
33. Dillon, M. E. *et al.* Life in the Frequency Domain: the Biological Impacts of Changes in Climate Variability at Multiple Time Scales. *Integr. Comp. Biol.* **56**, 14–30 (2016).
34. Adamo, S. A., Baker, J. L., Lovett, M. M. E. & Wilson, G. Climate Change and Temperate Zone Insects: The Tyranny of Thermodynamics Meets the World of Limited Resources. *Environmental Entomology* **41**, 1644–1652 (2012).
35. Kingsolver, J. G., Diamond, S. E. & Buckley, L. B. Heat stress and the fitness consequences of climate change for terrestrial ectotherms. *Functional Ecology* **27**, 1415–1423 (2013).
36. Dillon, M. E., Wang, G. & Huey, R. B. Global metabolic impacts of recent climate warming. *Nature* **467**, 704–706 (2010).
37. Sunday, J. M. *et al.* Thermal-safety margins and the necessity of thermoregulatory behavior across latitude and elevation. *PNAS* **111**, 5610–5615 (2014).
38. Pincebourde, S. & Casas, J. Narrow safety margin in the phyllosphere during thermal extremes. *Proc Natl Acad Sci USA* **116**, 5588–5596 (2019).
39. Johansson, F., Orizaola, G. & Nilsson-Örtman, V. Temperate insects with narrow seasonal activity periods can be as vulnerable to climate change as tropical insect species. *Sci Rep* **10**, 8822 (2020).
40. Davis, A. J., Jenkinson, L. S., Lawton, J. H., Shorrocks, B. & Wood, S. Making mistakes when predicting shifts in species range in response to global warming. *Nature* **391**, 783–786 (1998).
41. Suttle, K. B., Thomsen, M. A. & Power, M. E. Species Interactions Reverse Grassland Responses to Changing Climate. *Science* **315**, 640–642 (2007).
42. Gouhier, T. C., Guichard, F. & Menge, B. A. Ecological processes can synchronize marine population dynamics over continental scales. *Proceedings of the National Academy of Sciences* **107**, 8281–8286 (2010).
43. Harley, C. D. G. Climate Change, Keystone Predation, and Biodiversity Loss. *Science* **334**, 1124–1127 (2011).
44. Gouhier, T. C., Grinsted, A. & Simko, V. *biwavelet: Conduct Univariate and Bivariate Wavelet Analyses*. (2021).
45. Huey, R. B. & Stevenson, R. D. Integrating Thermal Physiology and Ecology of Ectotherms: A Discussion of Approaches. *Am Zool* **19**, 357–366 (1979).

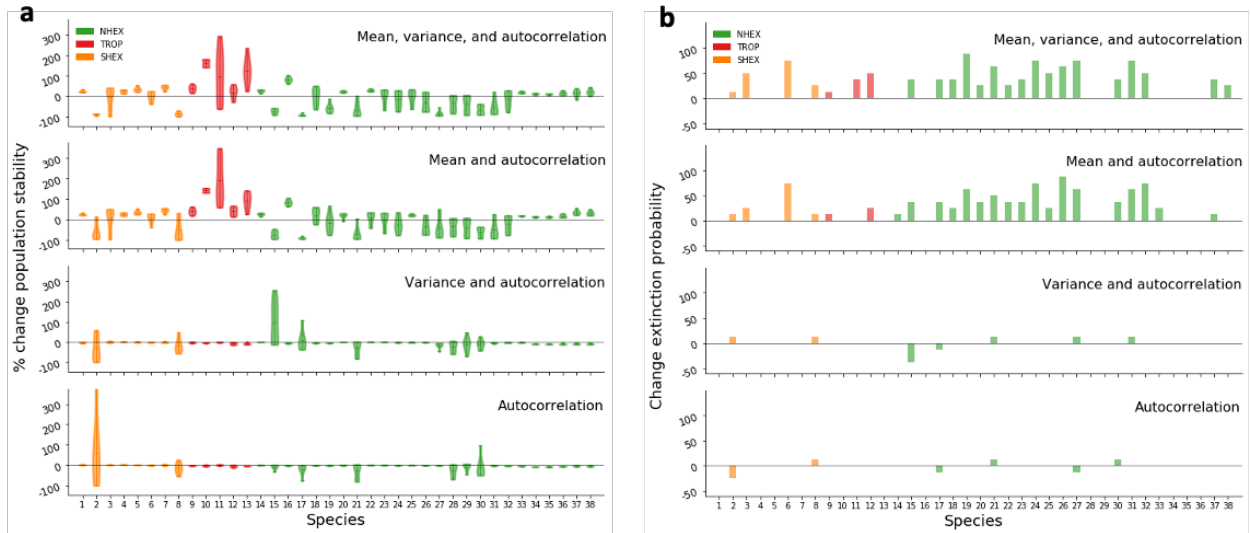
46. Mallet, J. The struggle for existence: how the notion of carrying capacity, K , obscures the links between demography, Darwinian evolution, and speciation. *Evolutionary Ecology Research* **14**, 627–665.

Extended Data



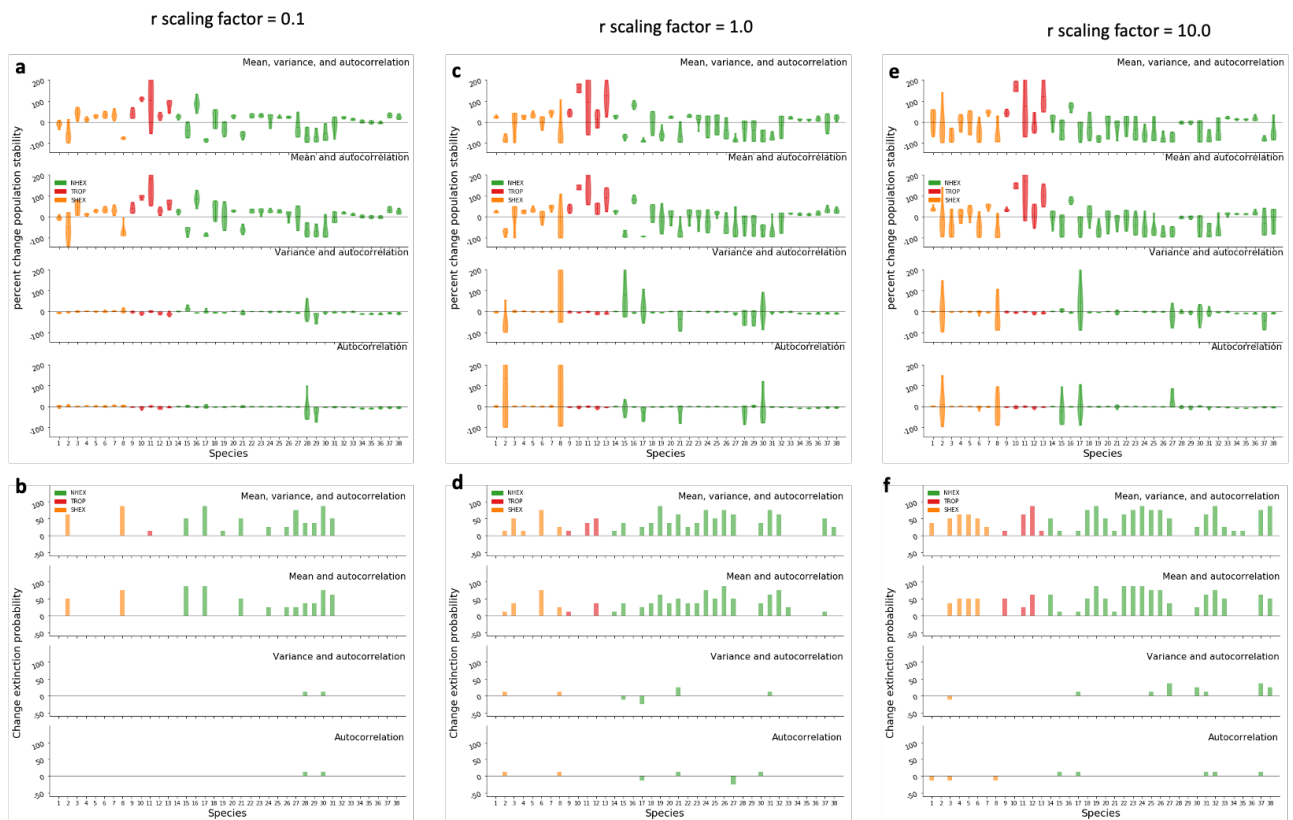
Extended Data Fig 1. Temperature variation at multiple timescales contributes to trends in overall variance.

a-b Trends in the power of variation at annual (3-days to 2-years) (a), inter- to multi-annual (2-30 years) (b) timescales between 1850 and 2100 suggest changes in the overall frequency spectrum of temperature variation. Countervailing trends are found in the Arctic, where the power of short fluctuations is decreasing and the power of persistent, low-frequency fluctuations is increasing.



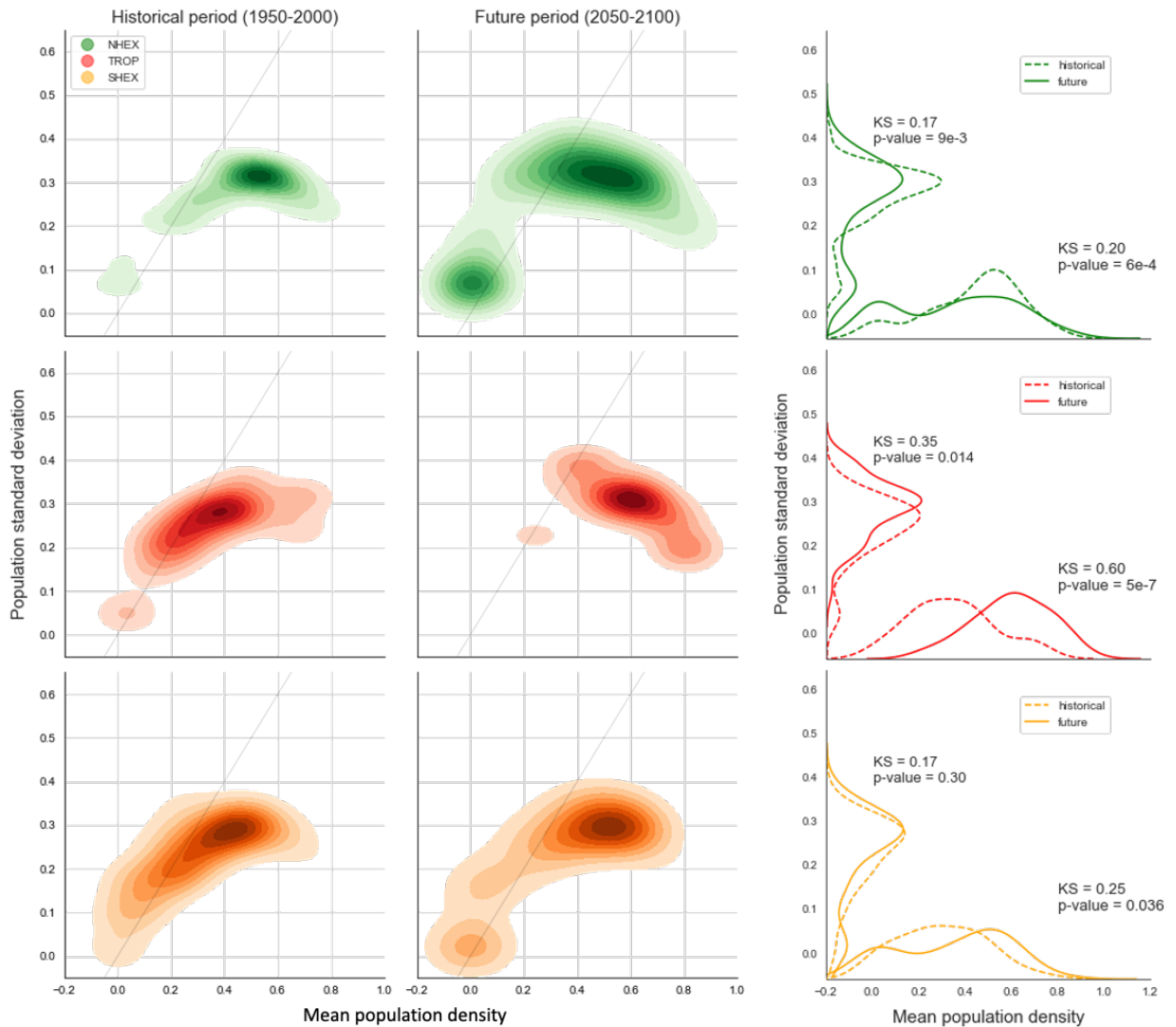
Extended Data Fig 2. Temperature-driven effects on population stability and extinction risk are robust to the degree of population self-regulation.

Results exhibited limited sensitivity to strong ($\alpha = 1$; Fig. 4) and weak ($\alpha = 0.1$; above) self-regulation in the form of crowding effects. Latitudinal patterns and effect sizes were consistent for changes in population stability, a, and extinction probability, b.



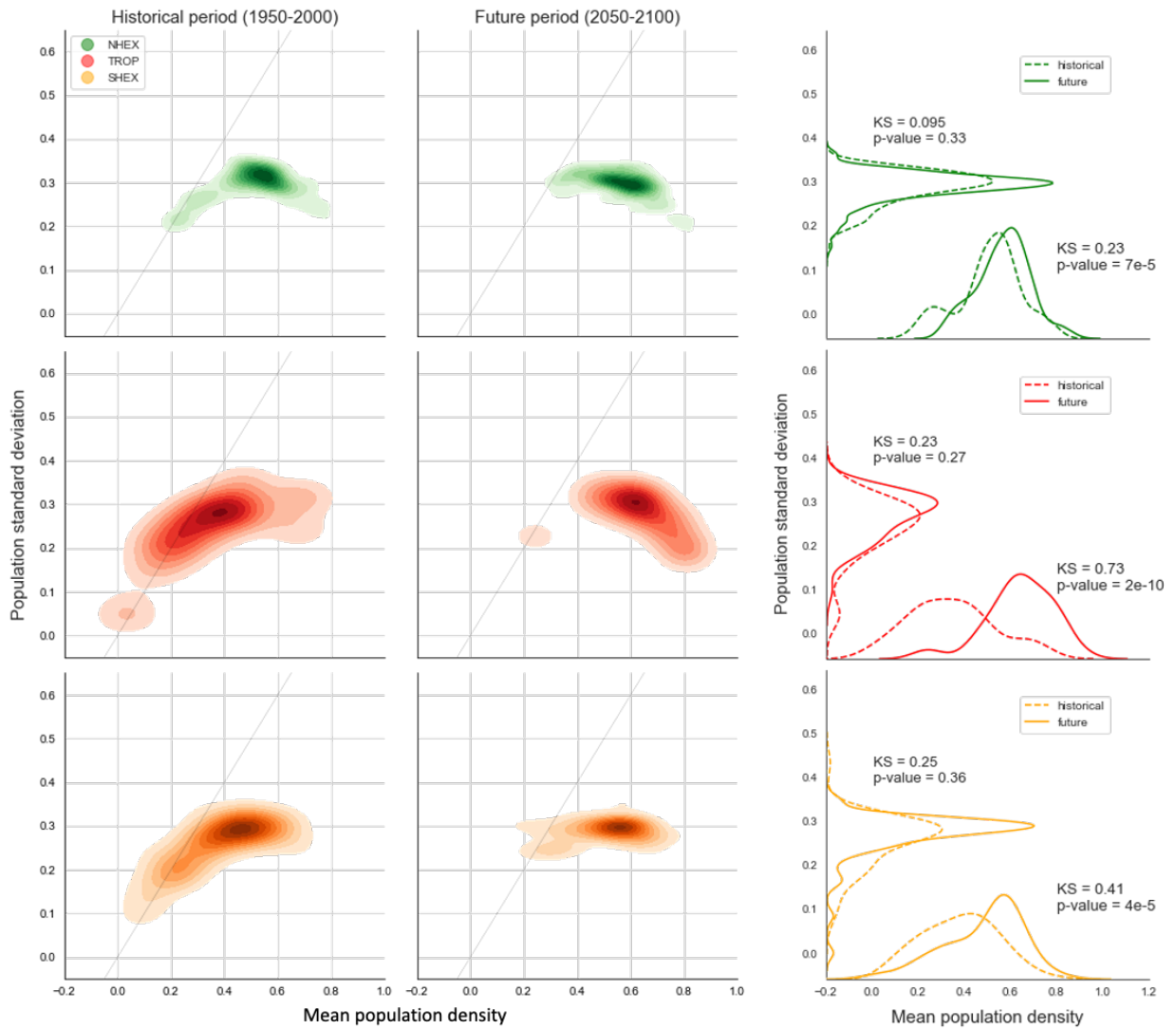
Extended Data Fig 3. Scaling of the intrinsic growth rate has moderate effects on temperature-driven impacts on population stability and extinction risk.

Results exhibited limited sensitivity to the choice of smaller (scaling factor = 0.1; **a,b**) and larger (scaling factor = 10.0; **e,f**) intrinsic growth rates. Although larger growth rates were more strongly associated with decreased stability and increased extinction risk than smaller growth rates, the latitudinal patterns and effect sizes were consistent with the changes in population stability, **c**, and extinction probability, **d**, observed under normalized growth rates.



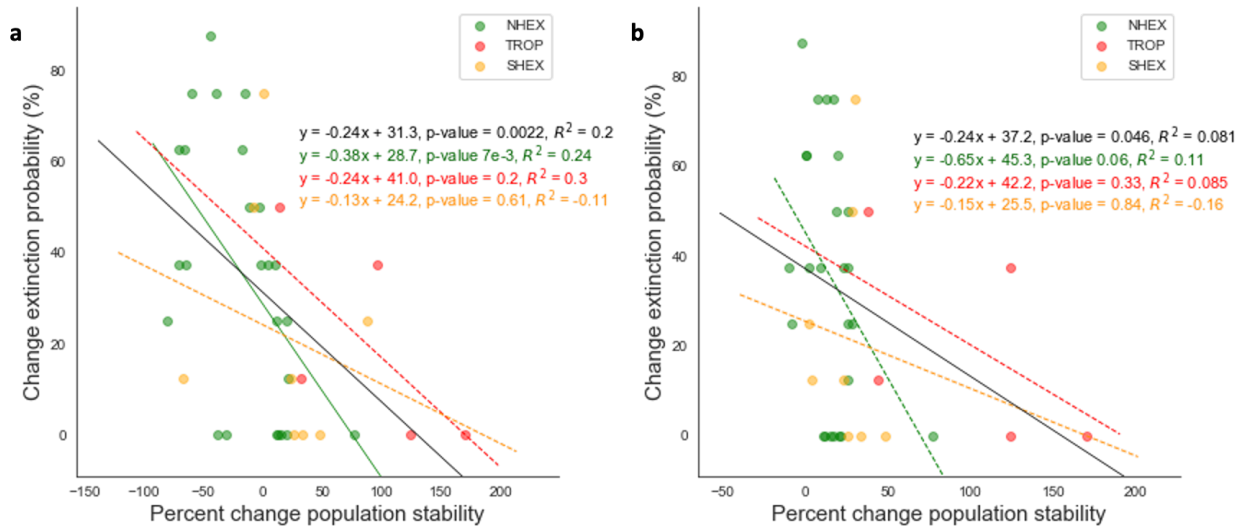
Extended Data Fig 4. Drivers of changes in stability (analysis includes both pre- and post-extinction period).

Kernel density plots illustrate the relationships between population mean and population standard deviation in the historical period and the future climate change period. The grey 1:1 line divides the more stable regime (high-mean/low-variance; below line), and the less stable regime (low-mean/high-variance; above line). Bimodal distributions emerge in the extra-tropics, with some species at low abundance and standard deviation, and a larger cluster of species at high abundance and standard deviation. In the tropics, the emergence of two regimes is associated with significant increases in the distributions of both population abundance and standard deviation via the Kolmogorov-Smirnov test.



Extended Data Fig 5. Drivers of changes in stability (analysis only includes pre-extinction period).

Although narrower distributions result for mean and standard deviation when only pre-extinction dynamics are analyzed, changes in the general patterns of stability regimes are consistent. Statistically significant changes in population abundance persist in all three regions; changes in population standard deviation become (remain) non-significant for NHEX and TROP (SHEX).



Extended Data Fig 6. Increased stability is negatively related to extinction probability.

Regression relationships in our simulations are presented **a**, when considering only the pre-extinction time period and **b**, when taking into account the full 50-year periods. Regardless of largely positive (**b**) or mixed (**a**) changes in stability, there is generally a weak but significant negative relationship between stability and extinction probability globally (p-value < 0.05).

Extended Data Table 1. Multimodel mean trends and in the spectral exponent of air temperature and statistical significance. Trends were estimated via Generalized Least Squares regression.

	All locations			Land			Sea		
	Slope (E-3)	Intercept	p-value	Slope (E-3)	Intercept	p-value	Slope (E-3)	Intercept	p-value
GLOBAL	-0.54	-1.29	0.005	-0.88	-1.28	0.008	-0.47	-1.30	0.002
NHEX	-1.12	-1.28	0.012	-1.67	-1.27	0.007	-0.88	-1.28	0.012
TROP	-1.14	-1.41	0.001	-1.42	-1.38	0.002	-1.04	-1.42	<0.001
SHEX	0.533	-1.19	0.009	0.412	-1.16	0.010	0.499	-1.19	0.025

Extended Data Table 2. Analysis of covariance (ANCOVA) was used to detect statistically significant effects of environment category (land and sea) on the relationship between spectral exponent and time. Nonsignificant interactions (SHEX) indicate similar regression relationships between spectral exponent and time in both environments. Significant interaction (GLOBAL, NHEX TROP; bolded) indicates a dissimilar regression relationship in sea and land environments. Autocorrelation is increasing at a greater rate with respect to time at NHEX terrestrial locations than NHEX marine locations.

	Time		Category		Interaction	
	F(1, 46)	p-value	F(1, 46)	p-value	F(1, 46)	p-value
GLOBAL	97.6	<0.001	402	<0.001	7.15	0.010
NHEX	62.2	<0.001	12.6	<0.001	4.77	0.034
TROP	218	<0.001	642	<0.001	4.90	0.032
SHEX	25.7	<0.001	429	<0.001	0.114	0.730

Extended Data Table 3. Number of species that experience a statistically significant increase (↑), a statistically significant decrease (↓), and no significant change (—) in population abundance under each of the four climate scenarios. Significant inter-model agreement on the direction and significance of change at the alpha=0.1 level.

		Autocorrelation			Variance and autocorrelation			Mean and autocorrelation			Mean, variance and autocorrelation		
		↑	↓	—	↑	↓	—	↑	↓	—	↑	↓	—
Population abundance	NHEX (n=25)	0	0	25	0	2	23	9	8	8	8	8	9
	TROP (n=5)	0	0	5	0	0	5	5	0	0	5	0	0
	SHEX (n=8)	0	0	8	0	0	8	5	1	2	5	2	1
	GLOBAL (n=38)	0	0	38	0	2	36	19	9	10	18	10	10
Population stability	NHEX (n=25)	0	3	22	0	5	20	10	8	7	8	8	9
	TROP (n=5)	0	0	5	0	0	5	5	0	0	4	0	1
	SHEX (n=8)	0	0	8	0	0	8	4	1	3	4	2	2
	GLOBAL (n=38)	0	3	35	0	5	33	19	9	10	16	10	12